Research Article

Received: 16 July 2009 Revised: 19 June 2010 Accepted: 24 September 2010 Published online in Wiley Online Library: 21 January 2011

(wileyonlinelibrary.com) DOI 10.1002/pi.3011

Protein adsorption materials based on conducting polymers: polypyrrole modified with ω-(*N*-pyrrolyl)-octylthiol

Zhihong Zhang,* Yan Liang, Ping Liang, Chao Li and Shaoming Fang*

Abstract

In order to fabricate a new polymer matrix for application in biochips and to understand the mechanism of adsorption of proteins on conducting polymers, we prepared polypyrrole (PPy) functionalized with ω-(*N*-pyrrolyl)-octylthiol moieties. The chemical structure of the polymer could be controlled by varying the concentration of pyrrole added as the monomer. Initially, ω-(*N*-pyrrolyl)-octylthiol was self-assembled into a monolayer on a gold surface. Thereafter, a layer of uniform and smooth PPy was obtained by the chemical copolymerization of pyrrole and the ω-(*N*-pyrrolyl)-octylthiol. Bovine serum albumin (BSA) adsorption on the polymer was investigated using surface plasmon resonance spectroscopy and cyclic voltammograms. The chemical structure and monomer components of the as-prepared films were characterized using Fourier transform infrared spectroscopy and X-ray photoelectron spectroscopy. Water contact angle measurements were used to assess the surface wettability of the films throughout the preparative procedure. The kinetics of BSA adsorption onto the polymer could be controlled by varying the copolymer thickness and the pH value of the buffer solutions used. Moreover, the electroactivity was changed upon BSA binding. The results suggest that the new conducting polymer may potentially be applied as a more sensitive and reliable matrix in protein sensors.

Keywords: bovine serum albumin; surface plasmon resonance spectroscopy; polypyrrole; protein adsorption

INTRODUCTION

Recently, many kinds of organic surfaces, such as self-assembled monolayers (SAMs),[1,2] plasma-modified polymerization surfaces,[3–7] polymer brushes obtained by atom-transfer radical polymerization[8,9] and conducting polymers (CPs),[10–14] have been fabricated for protein adsorption with a view to developing new biomaterials, biological assays and biosensors. In particular, CPs have attracted considerable attention for such applications due to their good overall properties. Mainly due to its stability, conductivity and biocompatibility, polypyrrole (PPy) has been the most extensively investigated and widely used material for biosensors.[15–18] Although CPs can be directly deposited on electrodes by electrochemical polymerization[19–21] or on substrates by *in situ* polymerization,[22–24] the two layers are not bonded together chemically. Stresses at the interface, such as those caused by volume changes induced during doping/undoping of the polymer, can cause the layers to separate, which is the main cause of device failure in actuators.[25,26] PPy films can also be formulated using the method of plasma polymerization.[27–31] Thin and dense polymer layers of a desired chemical functionality may be deposited on virtually any surface without the use of solvents in a fast and cost-effective manner by plasma polymerization. When immersed in buffer solution, however, the solution behavior of plasma-formed polymers is not fully understood. Sometimes, they are not stable in aqueous solutions.[32,33]

Consequently, it is most important to form a stable, sensitive substrate allowing immobilization of highly concentrated biomolecules such as DNA, enzymes, antibodies or antigens with complete retention of their biological activity while permitting good accessibility for the target molecules.

The method of forming SAMs of alkylthiols on gold surfaces has been widely explored for use in applications requiring adhesion promotion. Hence, there have been many efforts to improve the adhesion of PPy to substrates. *N*-[3-(Trimethoxysilyl)propyl]pyrrole has been synthesized as a surface-modification agent to improve the adhesion of PPy films on *n*-type silicon through its covalent anchoring on the surface.[34] It has also been shown that photopatterning of such SAMs can be used to selectively deposit CPs.[35] Two layers were chosen to be chemically bound together by using a molecule containing both a sulfhydryl and a pyrrole group as a link between the polymeric phase and the supporting substrate.[36] Also, the electrochemical properties of a monolayer alone were investigated in detail in order to understand the effects of the monomer monolayer on the morphology of a bulk-deposited polymer following modification of PPy film properties using ω-(*N*-pyrrolyl)-alkanethiol/gold surfaces.[37] The chemistry associated with a series of ω-(*N*-pyrrolyl)-alkanethiol monolayers on gold and their effects on the nucleation and growth of PPy films have been studied. It was found that the PPy films

* *Correspondence to: Zhihong Zhang and Shaoming Fang, Henan Provincial Key Laboratory of Surface and Interface Science, Zheng Zhou University of Light Industry, No. 5 Dong Feng Road, Zheng Zhou 450002, China.*
E-mail: mainzhh@yahoo.com.cn; mingfang@zzuli.edu.cn

Henan Provincial Key Laboratory of Surface and Interface Science, Zheng Zhou University of Light Industry, No. 5 Dong Feng Road, Zheng Zhou 450002, China

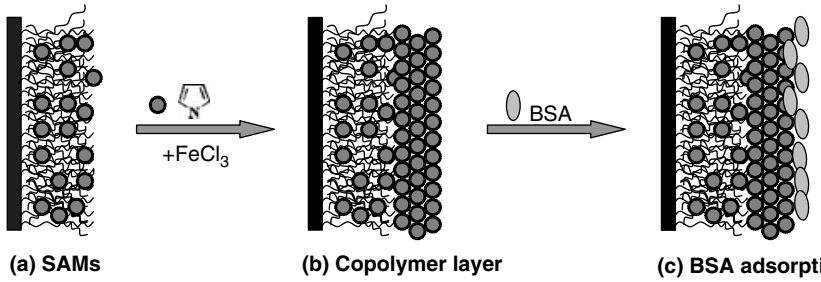

Figure 1. Schematic representation of (a) the preparation of ω-(*N*-pyrrolyl)-octylthiol SAM on a gold surface, (b) the chemical copolymerization of pyrrole with octylthiol-modified pyrrole and (c) the adsorption of BSA on the PPy surfaces.

formed on the ω-(*N*-pyrrolyl)-alkanethiol/gold surfaces were very adherent and extremely smooth when compared to PPy films formed on unmodified gold surfaces. The difference in polymer morphology could be attributed to enhanced nucleation.[38] Simon *et al*. concluded that the strong polymer adhesion observed for ω-(*N*-pyrrolyl)-alkanethiol/gold surfaces could only be due to coupling of the surface-confined pyrrole cation with pyrrole radical cations in solution, resulting in a covalently bound polymer film.[34] On the basis of these studies concerning SAMs containing pyrrole groups, it would appear that such CP films have attractive prospects for application as biomaterials. However, few papers on the immobilization or adsorption of biomolecules on such SAM films have been published.

The primary driving force of the interaction between protein molecules and PPy surfaces seems to be hydrophobic. Electrostatic contributions also play an important role, particularly for more hydrophilic surfaces. Furthermore, surface geometry and morphology are also likely to play a role. A further contribution to protein adsorption comes from van der Waals forces, although normally these are much smaller in magnitude. Therefore, the inherent properties of PPy films and proteins play an important role in the process of adsorption. Also, the properties of the buffer solutions used, e.g. their pH value, affect the adsorption behavior. All of these factors may contribute to determining the actual interaction of proteins with PPy.

In the work reported here, ω-(*N*-pyrrolyl)-octylthiol was synthesized using the method of Willicut and McCarley.[38] After self-assembly of a monolayer of ω-(*N*-pyrrolyl)-octylthiol on a gold film, a uniform and smooth PPy film of thickness < 50 nm was prepared by polymerization, the film being suitable for surface plasmon resonance (SPR) measurements.

EXPERIMENTAL

The whole experimental process is shown in Fig. 1. Three steps, namely the synthesis of ω-(*N*-pyrrolyl)-octylthiol, the *in situ* polymerization of PPy and the adsorption of bovine serum albumin (BSA) on PPy films, were conducted. BSA of molecular weight of 67 000 g mol^{-1} was purchased from Shanghai Biolife Science & Technology Co. Ltd, China. Pyrrole, KOH and dibromoalkanes were purchased from Aladdin, China. CSN_2H_4 was obtained from the factory of Sitong Tianjin, China. $FeCl_3$, diethyl ether, ethyl acetate, anhydrous magnesium sulfate and other chemicals were of analytical grade or better, and were used without further purification. The buffer used was 0.01 mol L^{-1} phosphate-buffered saline (PBS; pH = 7.4), and protein solutions were prepared by dilution with PBS. All solutions were prepared with deionized (DI) water from a Millipore Milli-Q water purification system.

Table 1. Preparation of PBS of various pH

pH	4.9	5.6	6.6	7.4	8.0
A (mL)	0.1	0.5	4.0	8.0	9.5
B (mL)	9.9	9.5	6.0	2.0	0.5

Protein solutions were stored at 4 °C prior to use. Thin gold films (47–50 nm) for SPR measurements, prepared by thermal evaporation, were purchased from the Institute of Electronics, Chinese Academy of Sciences. Clean gold substrates were dipped into a freshly prepared H_2SO_4/H_2O_2 piranha solution (7 : 3 v/v) for 3 min and then rinsed with DI water from the Milli-Q system. [Caution: these solutions are highly oxidizing and should be handled with extreme care.] Buffer solutions of various pH values were prepared from solutions A and B in the ratios shown in Table 1. An EC-PH510 pH meter (Singapore) was used to measure the pH of buffer solutions.

Monolayer and PPy film formation

Gold substrates were rinsed with pure ethanol and then incubated in 1 mmol L^{-1} solutions of ω-(*N*-pyrrolyl)-octylthiol in absolute ethanol for at least 24 h. After self-assembly of the ω-(*N*-pyrrolyl)-octylthiol (Fig. 1(a)), the samples were rinsed with copious amounts of ethanol and allowed to dry in nitrogen. The PPy film was polymerized in a methanolic solution of 1.5×10^{-3} mol L^{-1} pyrrole and 1.5 mol L^{-1} $FeCl_3$ and then rinsed with a large volume of methanol and dried by exposure to the atmosphere (Fig. 1(b)). The thickness of the PPy film could be controlled by adjusting the polymerization time, which was varied from 1 to 4 min.

Preparation of PBS solutions

Solution A was composed of 9.465 g of $Na_2HPO_4 \cdot 12H_2O$ dissolved in 1000 mL of DI water. Solution B was composed of 9.07 g of KH_2PO_4 dissolved in 1000 mL of DI water. Solutions A and B were stored at 4 °C in brown bottles. They were mixed together in various proportions to produce PBS of various pH values (Table 1).

Spectral analyses

Fourier transform infrared (FTIR) spectra of pure PPy films were recorded from samples in KBr pellets with a Nicolet 5700 FTIR spectrometer (Thermo Electron Corporation). The spectra were recorded from 4000 to 400 cm^{-1}, with a resolution of 4 cm^{-1} for 32 scans.

X-ray photoelectron spectroscopy (XPS) measurements were made with a Kratos AXIS HSi spectrometer using a monochromatized Al-K X-ray source (1486.71 eV photons) with a pass energy

of 40 eV. Samples were mounted on the sample studs with the aid of double-sided adhesive tape. XPS signals were obtained at a photoelectron take-off angle of 90° (with respect to the sample surface). The X-ray source was run at a power of 150 W (15 kV and 10 mA). The pressure in the analysis chamber was maintained at or below 10^{-8} torr (1.3×10^{-6} Pa) during each measurement. All binding energies were referenced to the C 1s hydrocarbon peak at 284.6 eV. Surface elemental stoichiometries were determined from XPS area ratios, after correcting using the experimentally determined sensitivity factors. Peaks in the elemental core-level spectra were fitted using commercial XPS analysis software. The number of peaks chosen for each fit was the minimum number required to obtain random residuals. A linear function was used to model the background, with the corresponding coefficients being fitted simultaneously with the peaks.

SPR measurements

A glass slide covered with gold film suitable for the SPR apparatus (SPR 2005, Electronic Institute of the Chinese Academy of Sciences) was pressed onto the base of a half-cylindrical lens ($n = 1.61$) using an index-matching oil. Linearly p-polarized light with a wavelength of 670 nm from a diode laser was directed through a prism onto the gold film in the Kretshmann configuration.[39] The intensity of the reflected light was measured as a function of the angle of incidence, θ, using a photodiode with a chopper/lock-in amplifier technique. For SPR detection, the as-prepared gold/glass substrates were mounted against a Teflon cuvette of volume 1 mL using a Kalrez O-ring, which provided a liquid-tight seal. The baseline of the SPR binding curve was obtained after injecting buffer, i.e. 0.01 mol L^{-1} PBS (pH = 7.4), into the cuvette. In particular, in order to investigate the influence of pH, buffer solutions of pH = 4.9, 5.6, 7.4 and 8.0 were used. After obtaining a stable baseline, protein solution was added in place of the buffer solution. After measuring the binding curve, the solution was changed back to the buffer once more. All experiments were conducted at room temperature.

The de Feijter formula[39] expressed as

$$\Gamma = \frac{d_f(n_f - n_{buffer})}{dn/dc} \quad (1)$$

was used to quantify the adsorbed weight Γ (mg m^{-2}) from the film thickness (d_f, expressed in nm), the refractive index of the film (n_f) and the refractive index of the buffer (n_{buffer}). A dn/dc value of 0.18 mL g^{-1} was used for the calculations. The SPR instrument expresses the shift in θ as resonance units (RU). The RU contains a calibration constant that converts shifts in θ to adsorbed amount (μg m^{-2}). It has been found that 1 RU corresponds to 1 μg m^{-2} for protein molecules.[40,41] The refractive index for BSA used here was 1.45.[42] The refractive index of buffer solution was in the range 1.33–1.34. Hence, d_f can be calculated using

$$d_f \text{ (nm)} \approx 1.5\Gamma \quad (2)$$

which is deduced from Eqn (1) if the weight of adsorbed protein is estimated.

Contact angle measurements

Contact angles were determined with a contact angle instrument (SL 200B, Solon Tech Co. Ltd, Shanghai, China) at room temperature and 100% relative humidity for water and ambient humidity for all other probe liquids. Under these conditions, the contact angles were stable for 3 minutes. The advancing water contact angle, θ (air) H_2O, was obtained by forming a 2 μL drop of water at the end of a polytetrafluoroethylene-coated blunt-ended needle attached to a 50 μL syringe fitted with a repeater, lowering the needle until the drop touched the surface, and raising the needle. As the drop was detached from the needle tip, it advanced over the surface. Each determination was performed by averaging the results obtained for at least five droplets.

RESULTS AND DISCUSSION

Characterization of chemical structure using FTIR and XPS analyses

FTIR spectra of ω-(*N*-pyrrolyl)-octylthiol on a gold film and PPy are shown in Fig. 2. Figure 2(a) shows the FTIR spectrum obtained after the self-assembly of ω-(*N*-pyrrolyl)-octylthiol on a gold film. Since the monolayer of ω-(*N*-pyrrolyl)-octylthiol is thin, the FTIR signal intensity is rather weak. Nevertheless, some peaks can be identified. The peak at 1263 cm^{-1} may be attributed to the =N– group of the ω-(*N*-pyrrolyl)-octylthiol, supporting its self-assembly on the gold film. Figure 2(b) shows the FTIR spectrum of a PPy film prepared by polymerization for 5 min. The broad peak at 3440 cm^{-1} may be ascribed to the unsaturated $\nu(N-H)_{ring}$ vibration of the pyrrole ring. The peaks at 2930 and 2860 cm^{-1} may be assigned to the saturated $\nu_a(CH_2)$ and $\nu_s(CH_2)$, respectively. The peak at 1500 cm^{-1} may be attributed to a characteristic in-plane C=C stretching vibration of the pyrrole ring, while that at 1090 cm^{-1} may be ascribed to –C–N– of the alkanes. The symmetric out-of-plane C–H deformation $\omega_s(C-H)_{ring}$ appears near 720 cm^{-1}.

The C 1s, N 1s and S 2p core-level XPS spectra of a SAM film and a PPy film prepared for 5 min are shown in Fig. 3. The C 1s spectra of both SAM and PPy can be divided into a component peak at 284.2 eV, attributable to the $C-C/CH_x$ groups, a higher binding energy peak (285.4 eV) due to C–O/C–N groups and a lower intensity peak at 287.8 eV due to the HN–C=O groups. As regards the N 1s spectra, in comparison with the PPy film, only weaker N 1s signals of the SAM can be detected. The N 1s spectra can be fitted with four peaks, i.e. a main component peak at 399.3 eV attributable to the $C-N/NH_x$ groups, a higher binding energy peak (400.5 eV) due to the O=C–N–C=O moiety, a higher binding energy tail at 401.5 eV attributable to the positively charged nitrogen ($-N^+-$) and a lower binding energy peak (397.5 eV) due to the =N– groups. In the case of the SAM film, a substantial S 2p signal is measured, confirming that the ω-(*N*-pyrrolyl)-octylthiol had been self-assembled on the gold surface. In contrast, after pyrrole monomer is polymerized on the SAM surface, a thick PPy layer is formed. Since the detection limit of XPS is only about 8–10 nm, an S 2p signal is no longer detected. Since the oxidation potential of PPy is lower than that of pyrrole monomer, the polymer could be simultaneously oxidized with pyrrole monomer in the course of the polymerization.[43] PPy is usually in its oxidized state and bears charges in the polymer matrix, i.e. some of the nitrogen atoms in PPy are positively charged. These positive charges in the polymer are amenable to some applications involving the adsorption of biomolecules due to electrostatic interactions.

Surface wettability

Contact angles on gold, SAM and PPy films polymerized for different times, i.e. 1, 2, 3 and 4 min, are shown in Fig. 4. After cleaning with ethanol, the gold surface bears many hydroxyl

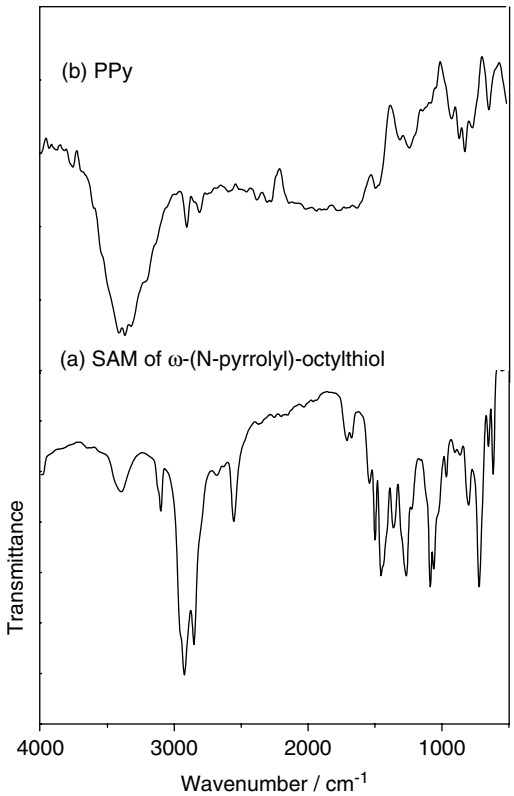

Figure 2. FTIR spectra of (a) ω-(*N*-pyrrolyl)-octylthiol and (b) PPy film polymerized for 5 min. All samples were on gold surfaces.

groups. Therefore, its contact angle is less than that on the self-assembled ω-(*N*-pyrrolyl)-octylthiol film. When ω-(*N*-pyrrolyl)-octylthiol self-assembly (SAM) is complete, the pyrrole groups exhibit hydrophobicity and extend from the gold surface to form a compact monolayer. Consequently, water molecules are repelled by the pyrrole groups, and the surface shows a higher contact angle.[44] On increasing the time of *in situ* polymerization from 1 to 4 min, the contact angle at the polymer surface increases from 78.6° to 87.2°. The monolayer of ω-(*N*-pyrrolyl)-octylthiol provides covalently bound organic nucleation sites on the surface for the deposition and growth of organic PPy chains. Hence, a complete molecular network is ultimately produced, resulting in a lowering of surface free energy. As a consequence, the contact angles of PPy films prepared for a longer time are higher. This would suggest that hydrophobic interactions play an important role in BSA adsorption. However, it is known that the driving force for adsorption of 'soft' proteins,[45,46] such as BSA, is related to structural rearrangements in the molecules that enable them to overcome the unfavorable conditions offered by an electrostatically repelling surface. To reveal the true adsorption mechanism, it is necessary to investigate the real-time adsorption of BSA onto the PPy films in buffer solutions of varying pH.

Scanning of incident angle by SPR

The scan curves of incident angles on gold, SAM and PPy films, and BSA adsorbed on PPy are shown in Fig. 5. After self-assembly of the ω-(*N*-pyrrolyl)-octylthiol on the gold film, the deep angle of the SPR curve increases by about 0.3°, which is obtained using the fitting software. This suggests that the optical thickness of the layered media, i.e. gold and SAM on the glass substrates, is greater than before. Additionally, the shape of the SPR curve becomes broader, which could be due to the imaginary part of the refractive index of the ω-(*N*-pyrrolyl)-octylthiol monolayer.[47] When the polymerization is complete, the SPR angle shifts to an even higher value, suggesting that the optical thickness of the PPy film increases with time. Moreover, the shape of the SPR curve becomes much broader, which could result from the surface morphology of the PPy film becoming rougher with increasing polymerization time.[48]

In order to ensure reliable results in measurements of BSA adsorption on the PPy film, the film thickness was controlled such that it did not exceed 50 nm. This is exemplified by curves (c) and (d) of Fig. 5, which represent PPy films before and after full swelling. When the PPy film is immersed into a PBS solution, the backbone of the polymer will swell and the unpolymerized pyrrole monomer will be washed away. Once these two events reach a balance, the PPy film is in a stable state, as shown in curve (d). After introducing 1 vol% BSA solution into the system, curve (e) is the scan curve of BSA adsorption on the PPy film. A higher deep angle is again obtained, indicating that another layer is produced when the BSA is adsorbed. To fully understand the behavior of BSA adsorption on PPy films, a kinetic scan of SPR was obtained, as described below.[49]

BSA adsorption

In order to understand the importance of adsorption kinetics for PPy films, *in situ* SPR measurements were conducted for BSA adsorption on the films. BSA is a globular protein with a molecular weight of 67 000 g mol^{-1} and a pI (isoelectric point) of 4.7. Since its amino acid sequence and physical properties are well characterized, BSA has been widely used as a model protein. Generally, there are two extreme orientations for the adsorption

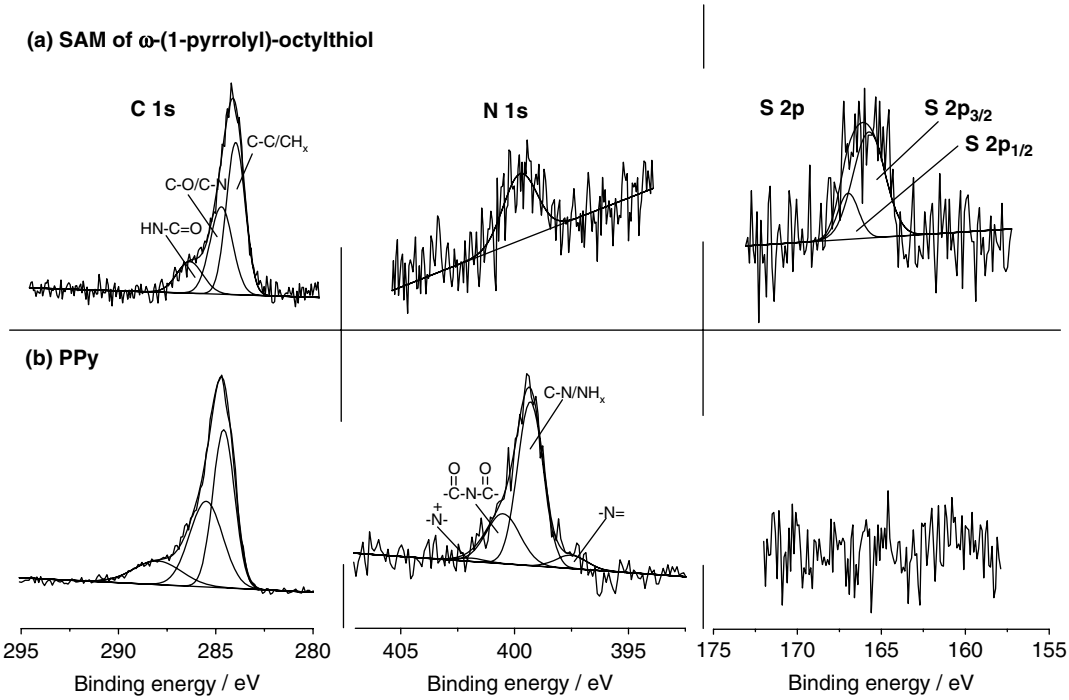

Figure 3. XPS spectra of (a) ω-(*N*-pyrrolyl)-octylthiol and (b) PPy film polymerized for 5 min on gold surface.

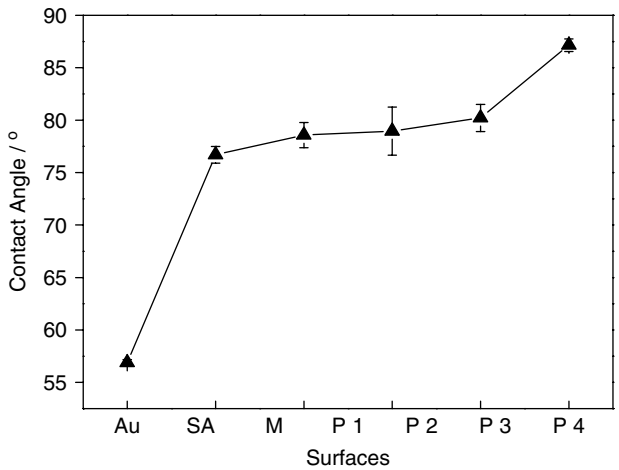

Figure 4. Contact angles of ω-(*N*-pyrrolyl)-octylthiol and PPy films. (P1, P2, P3 and P4 refer to PPy surfaces prepared with polymerization times of 1, 2, 3 and 4 min, respectively).

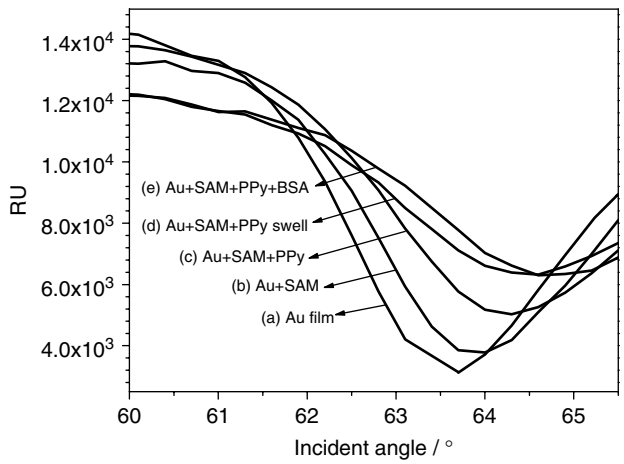

Figure 5. SPR responses of (a) bare gold film, (b) ω-(*N*-pyrrolyl)-octylthiol, (c) PPy film, (d) PPy film which are stable in PBS solution and (e) after BSA adsorption on the PPy film.

of BSA molecules onto a surface, i.e. side-on and end-on. Normally, it is adsorbed in a mixture of these orientations.

BSA adsorption behavior of SAM and PPy films

Once the PPy films reached equilibrium in the PBS buffer, the proteins were incubated in the SPR flow cell and the optical properties of the interface were monitored using SPR over time periods of at least 1 h. The kinetic curves of BSA adsorption behavior on SAM and PPy films prepared for 2, 3 and 4 min are shown in Fig. 6. For all samples studied, protein physisorption reaches equilibrium within a few minutes of injecting the protein into the cell. The systems were allowed to stabilize over a period of 1 h, but show no further significant changes. After this stabilization period, the samples were rinsed with excess PBS, which invariably leads to some loss of unbound protein from the surface of each PPy film.

The different adsorption behaviors on PPy films of thicknesses of 21, 35 and 48 nm were studied using polymerization times of 2, 3 and 4 min, respectively. According to the relationship between the reflectivity units of SPR and the adsorbed amounts or thickness of BSA, i.e. Eqns (1) and (2), after being rinsed with PBS buffer, the simulated adsorbed amounts and thickness of BSA onto all surfaces are summarized in Table 2. Compared with the SAM, a larger amount of BSA adsorbed on the polymer film is observed after 2 min of polymerization, as shown in Fig. 6. However, the amount of BSA adsorbed on PPy films decreases quickly after 3 and 4 min of polymerization.

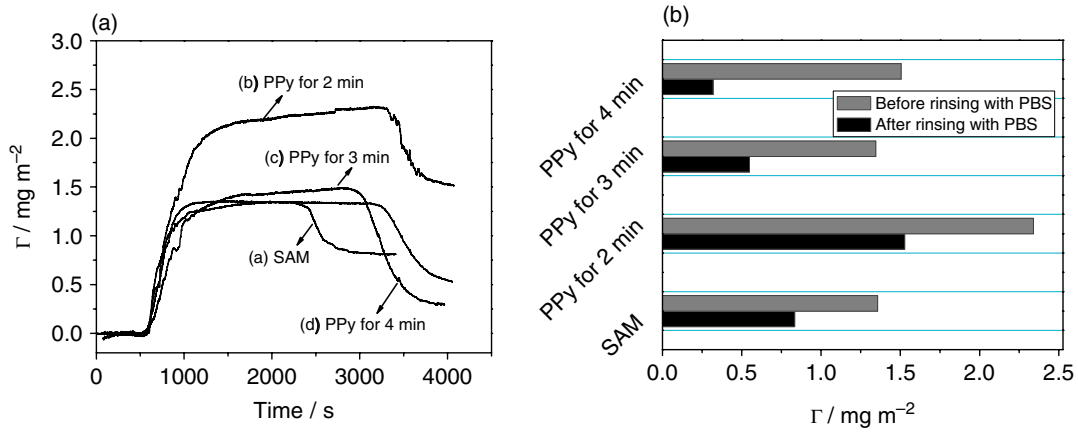

Figure 6. SPR binding curves of BSA on ω-(*N*-pyrrolyl)-octylthiol SAM and PPy films with various polymerization times.

Table 2. After being rinsed with PBS, the amounts adsorbed and thickness of adsorbed BSA on the surfaces of SAM and PPy films for various polymerization times

Surface for BSA adsorption	Amount of BSA adsorbed (g m^{-2})	Thickness of adsorbed BSA (nm)
SAM	0.83	1.25
PPy (2 min)	1.53	2.29
PPy (3 min)	0.53	0.82
PPy (4 min)	0.32	0.48

The structure of BSA has been previously characterized using X-ray crystallography, showing it to be a globular protein with dimensions of approximately 8 nm by 4 nm. BSA of approximately 2 nm in thickness was adsorbed onto the SAM film initially. This suggests BSA molecules are adsorbed in side-on orientation and cannot cover the full surface (Fig. 7(a)). However, once the reaction between the pyrrole groups of the SAM and the added pyrrole monomer commences, the first propagation of the polymerization is focused only at certain points on the surface. After 2 min of polymerization, the PPy is inhomogeneously distributed on the surface such that the SAM surface cannot be fully covered. PPy molecules have enough space in which to stretch, as shown in Fig. 7(b). BSA molecules not only adsorb on the polymerized surface, but also on the surface of the SAM. This results in more protein molecules being anchored on the surface. Before being rinsed with a large quantity of PBS, approximately 2.5 mg m^{-2} BSA, i.e. 3.5 nm of BSA, is adsorbed onto the PPy film with a polymerization time of 2 min, while after being rinsed with PBS, some BSA molecules that adsorb physically on the surface are removed and only 1.53 mg m^{-2} BSA, i.e. 2.29 nm of BSA, is left, as shown in Fig. 6. In all cases, it is evident that BSA still keeps its side-on conformation upon binding onto PPy films because the adsorbed thicknesses of BSA on all surfaces are less than 4 nm, i.e. the least value of monolayer of binding BSA.

With increasing polymerization time, the whole surface of the film will be fully covered by PPy, which leads to a much denser PPy surface. The steric influence of pyrrole becomes much greater, resulting in less interaction between BSA and the surface. Hence, less BSA can adsorb onto this kind of surface (Fig. 7(c)). From the contact angle results (Fig. 4), the hydrophobicity of the surface increases with increasing polymerization time, indicating that more BSA molecules may be adsorbed on the PPy surface. Compared with the effect of the steric structure of PPy films on BSA adsorption, however, the hydrophobicity of the PPy film surface has a weaker effect.[38,44,50]

Influence of buffer pH on BSA adsorption

In aqueous solutions, protein adsorption is mainly affected by the properties of the polymer surface, such as the surface electric properties, which greatly depend on the pH of the solution. To further understand the adsorption mechanism of BSA on PPy films, films with a thickness of 21 nm that had been polymerized for 2 min were used to investigate the effect of buffer pH on BSA adsorption (Fig. 8). A clear trend is that the amount of adsorbed BSA increases as the pH increases from 4.9 to 7.4. The results can be attributed to the electrostatic interaction between the BSA molecules and the PPy film. The BSA molecule is negatively charged in buffers with pH $>$ 4.7, and positively charged in buffers with pH $<$ 4.7. The positively charged PPy film repels BSA molecules in buffers with pH $<$ 4.7 but attracts them in buffers with pH $>$ 4.7. This would suggest that the higher the buffer pH, the more BSA molecules will be absorbed on the PPy film.[51] However, in a buffer solution at pH = 8.0, the least amount of BSA is adsorbed on a PPy film. The reason may be that the BSA molecules undergo less structural unfolding at pH = 8.0, resulting in the negative BSA presenting a maximum number of positive groups, such as N-termini and lysine residues, towards the surface.[52] On the other hand, an increase in the solution pH will reduce the H^+ concentration and increase the OH^- concentration in the aqueous solution. This may lead to deprotonation of the protonated nitrogen atoms on PPy, thereby leading to a decrease in oxidation level.[53,54] Hence, the electrostatic interactions between BSA and PPy will be decreased, thereby accounting for the observed reluctance of BSA molecules to adsorb on PPy film in a buffer solution at pH = 8.0.

Electrical properties of PPy before and after BSA adsorption

Figure 9 shows the cyclic voltammograms of PPy copolymer with a thickness of 55 nm for 5 min polymerization before and after BSA adsorption. The cyclic voltammograms of PPy demonstrate slight reduction and oxidation peaks. This indicates that the polymer exhibits a relatively high electroactivity. After BSA binding, however, the chemical content of polymer with BSA in the composite electrodes changes, which results in the electroactivity attenuation because of the expected blocking properties of the BSA layer.

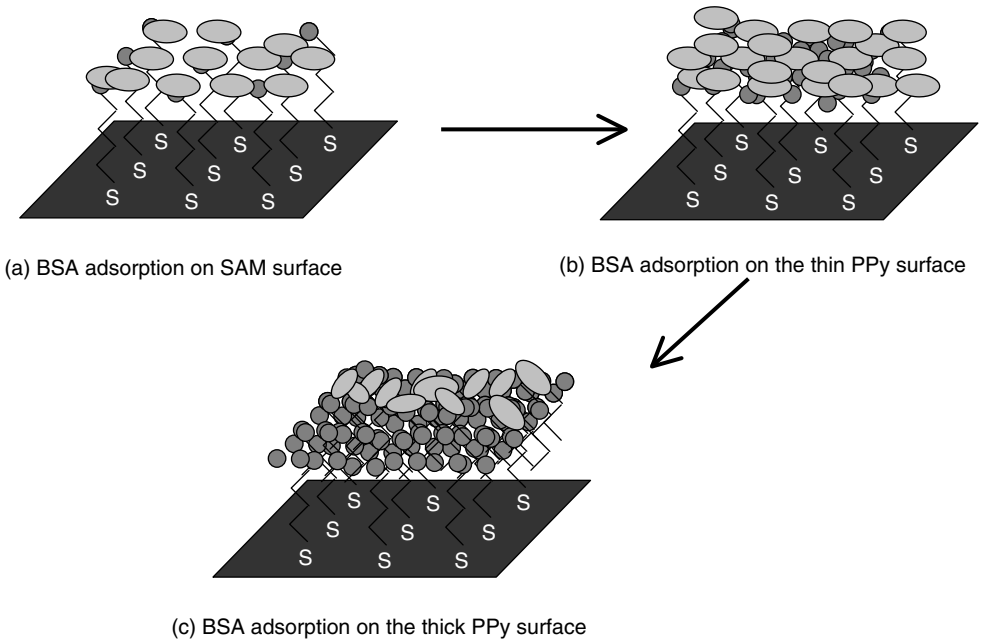

Figure 7. Schematic of BSA adsorption on SAM and PPy films prepared with times of 2, 3 and 4 min.

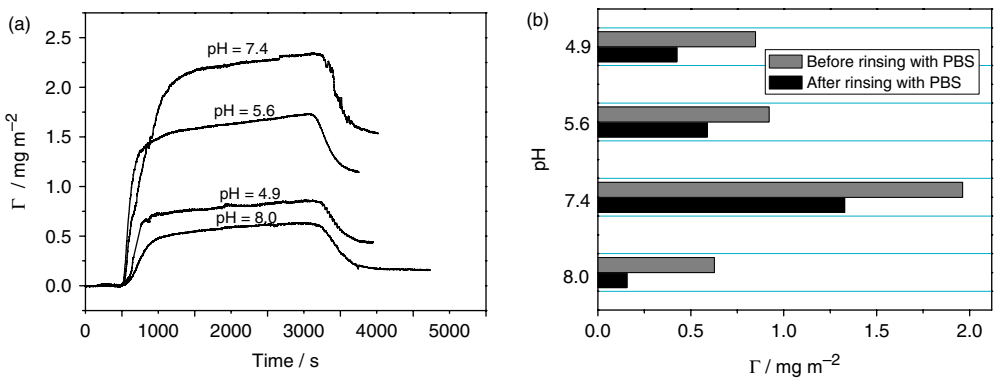

Figure 8. BSA adsorption on PPy films in buffer solutions of various pH.

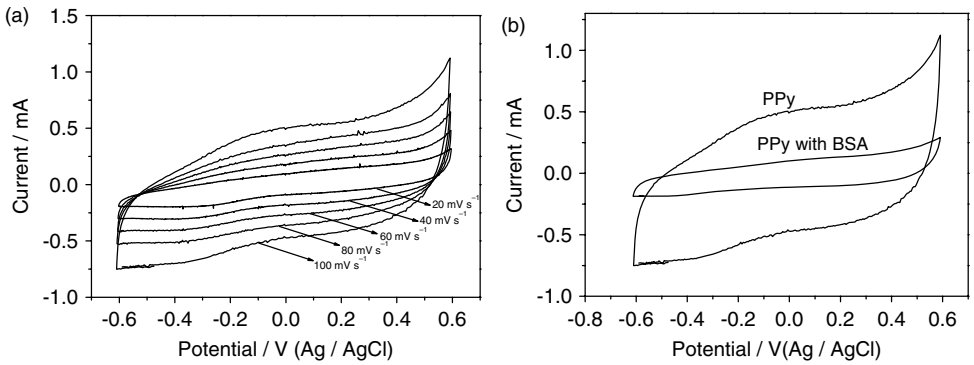

Figure 9. Cyclic voltammetry graphs of PPy film polymerized for 6 min (a) before and (b) after BSA adsorption. The scan rate used in (b) is 100 mV s^{-1}.

CONCLUSIONS

We have demonstrated that PPy films modified with ω-(*N*-pyrrolyl)-octylthiol may be prepared on gold surfaces. Trends in the adsorption behavior of BSA on PPy films have been observed from the SPR binding curves for SAM and PPy films (polymerized for 2, 3 and 4 min) and various pH values of the buffer solutions. Due to the steric effect of PPy films, the results concerning BSA adsorption on PPy films show that fewer BSA molecules are adsorbed on a thick polymer surface prepared for a longer polymerization time. In buffer solutions with pH $<$ 7.4, however, the amount of BSA adsorbed decreases with increasing pH. The least amount of BSA is adsorbed from a buffer solution at pH = 8.0. When the pH exceeds

4.7, the negatively charged BSA molecules are attracted by the positively charged PPy films by electrostatic interaction. Both the chemical structures or properties of the film and the properties of the buffer solution can affect the adsorption behavior of BSA on PPy films. In fact, the amount of BSA adsorbed to the polymer surface could be controlled by varying the polymerization conditions and the nature of the buffer solution. Additionally, due to the expected blocking properties of the BSA layer, the electroactivity of the composite electrodes before and after BSA adsorption is attenuated. Thus, the study of BSA adsorption in this work is deemed to be of significance for applications.

ACKNOWLEDGEMENTS

This work was supported by the Program for the National Natural Science Foundation of China (NSFC: account nos. 20704039 and 20871107) and the Program for Science and Technology Innovation Talents in Universities of Henan Province (HASTIT: no. 2010HASTIT023).

REFERENCES

1 Kim SJ, Gobi KV, Tanaka H, Shoyama Y and Miura N, *Sens Actuators B* **130**:281–289 (2008).
2 Mesthrige KW, Amro NA and Liu GY, *Scanning* **22**:380–388 (2000).
3 Gomathi N, Sureshkumar A and Neogi S, *Curr Sci* **94**:1478–1486 (2008).
4 MacDonald C, Morrow R, Weiss AS and Bilek MM, *J R Soc Interface* **23**:663–669 (2008).
5 Stine R, Cole CL, Ainslie KM, Mulvaney SP and Whitman LJ, *Langmuir* **23**:4400–4404 (2007).
6 Xue CY and Yang KL, *Langmuir* **23**:5831–5835 (2007).
7 Muguruma H, Kase Y, Murata N and Matsumura K, *J Phys Chem B* **110**:26033–26039 (2006).
8 Yoon KR, Ramaraj B, Lee SM and Kim DP, *Surf Interface Anal* **40**:1139–1143 (2008).
9 Xu FJ, Cai QJ, Li YL, Kang ET and Neoh KG, *Biomacromolecules* **6**:1012–1020 (2005).
10 Crombrugghe A, Yunus S and Bertrand P, *Surf Interface Anal* **40**:404–407 (2008).
11 Peng H, Soeller C and Sejdic JT, *Macromolecules* **40**:909–914 (2007).
12 Ramanavicius A, Kurilcik N, Jursenas S, Finkelsteinas A and Ramanaviciene A, *Biosens Bioelectron* **23**:499–505 (2007).
13 Kwon NH, Rahman MA, Won MS and Shim YB, *Anal Chem* **78**:52–60 (2006).
14 Arslan A, Kıralp S, Toppare L and Bozkurt A, *Langmuir* **22**:2912–2915 (2006).
15 Chen SJ, Chen W and Xue G, *Macromol Biosci* **8**:478–483 (2008).
16 Shirsat MD, Too CO and Wallace GG, *Electroanalysis* **20**:150–156 (2008).
17 Prabhakar N, Arora K, Singh SP, Pandey MK, Singh H and Malhotra BD, *Anal Chim Acta* **589**:6–13 (2007).
18 Ramanavicius A, Ramanaviciene A and Malinauskas A, *Electrochim Acta* **51**:6025–6037 (2006).
19 Mekhalif Z, Cossement D, Hevesi L and Delhalle J, *Appl Surf Sci* **254**:4056–4062 (2008).
20 Li Y, Zhang WX, Li GT and Ju Y, *Polymer* **49**:225–233 (2008).
21 Akinyeye R, Michira I, Sekota M, Ahmed AA, Baker P and Iwuoha E, *Electroanalysis* **18**:2441–2450 (2006).
22 Wang Y, Sotzing GA and Weiss RA, *Chem Mater* **20**:2574–2582 (2008).
23 Ferenets M and Harlin A, *Thin Solid Films* **515**:5324–5328 (2007).
24 Kharat HJ, Kakde KP, Savale PA, Datta K, Ghosh P and Shirsar MD, *Polym Adv Technol* **18**:397–402 (2007).
25 Smela E, Inganas O and Lundstrom I, *Science* **268**:1735–1738 (1995).
26 Smela E, Inganas O, Pei Q and Lundstrom I, *Adv Mater* **5**:630–632 (1993).
27 Zhang ZH, Liang P, Zheng XJ, Peng DL, Yan FF, Zhao R, *et al*, *Biomacromolecules* **9**:1613–1617 (2008).
28 Yague JL, Agulo N and Borros S, *Plasma Process Polym* **5**:433–443 (2008).
29 Sahin HT, *Centr Eur J Chem* **5**:824–834 (2007).
30 Takai O, Anita V and Saito N, *Surf Coat Technol* **200**:1106–1109 (2005).
31 Liu YC and Wang CC, *J Phys Chem B* **109**:5779–5782 (2005).
32 Zhang ZH and Feng CL, *Appl Surf Sci* **253**:8915–8922 (2007).
33 Zhang ZH and Feng CL, *J Biotechnol* **2**:743–751 (2007).
34 Simon RA, Ricco AJ and Wrighton MS, *J Am Chem Soc* **104**:2031–2034 (1982).
35 Rozsnyai LF and Wrighton MS, *J Am Chem Soc* **116**:5993–5994 (1994).
36 Smela E, Zuccarello G, Kariis H and Liedberg B, *Langmuir* **14**:2970–2975 (1998).
37 Collard DM and Sayre CN, *Polym Prepr* **35**:196–201 (1994).
38 Willicut RJ and McCarley RL, *Langmuir* **11**:296–301 (1995).
39 Kretschmann E, *Z. Physik* **241**:313–324 (1971).
40 de Feijter JA, Benjamins J and Veer FA, *Biopolymers* **17**:1759–1772 (1978).
41 Karlsson R and Stahlberg R, *Anal Biochem* **228**:274–280 (1995).
42 Stenberg E, Persson B, Roos H and Urbaniczky C, *J Colloid Interface Sci* **143**:513–526 (1991).
43 Zhang Z, Menges B, Timmons RB, Knoll W and Foerch R, *Langmuir* **19**:4765–4770 (2003).
44 Bredas JL and Street GB, *Acc Chem Res* **18**:309–315 (1985).
45 Wu CG, Chiang SC and Wu CH, *Langmuir* **18**:7473–7481 (2002).
46 Haynes CA and Norde W, *Colloids Surf B* **2**:517–566 (1994).
47 Norde W and Anusiem ACI, *Colloids Surf* **66**:73–80 (1992).
48 Guedon P, Livache T, Martin F, Lesbre F, Roget A, Bidan G, *et al*, *Anal Chem* **72**:6003–6009 (2000).
49 Kambhampati DK and Knoll W, *Curr Opin Colloid Interface Sci* **4**:273–280 (1999).
50 Bailey LE, Kambhampati D, Kanazawa KK, Knoll W and Frank CW, *Langmuir* **18**:479–489 (2002).
51 Liu ML, Zhang YY, Wang ML, Deng CY, Xie QJ and Yao SZ, *Polymer* **47**:3372–3381 (2006).
52 Hu WH, Li CM, Cui XQ, Dong H and Zhou Q, *Langmuir* **23**:2761–2767 (2007).
53 Arnebrant T, Ivarsson B, Larsson K, Lundstrom I and Nylander T, *Prog Colloid Polym Sci* **70**:62–66 (1985).
54 Zhang X and Bai R, *Langmuir* **19**:10703–10709 (2003).
55 de Marcos S and Wolfbeis OS, *Anal Chim Acta* **334**:149–153 (1996).

